AIAA JOURNAL
Vol. 37, No. 10, October 1999

Generation Mechanisms of Low-Frequency Centrifugal Fan Noise

K.-R. Fehse* and W. Neise†
DLR, German Aerospace Center, 10623 Berlin, Germany

Earlier investigations by Stahl and Argüello (Stahl, B., and Argüello, G., "Schallerzeugung und Schalldämpfung in einer Rohrströmung stromab einer unstetigen Querschnittserweiterung," *Acustica*, Vol. 65, No. 2, 1988, pp. 75–84), who studied the sound field in a circular duct generated by a jet flow, indicated that flow separation occurring in a diffuser attached to the jet nozzle leads to increased sound levels in the low-frequency regime. This observation formed the basis for the present study. Experiments were made with five centrifugal fan impellers. Cross-correlation studies involving the unsteady wall pressures in the impeller and the casing led to the following insights: the low-frequency noise of centrifugal fans is generated by classical flow separation regions located on the shroud and the blade suction sides of the impeller. The design of the shroud is of particular importance: a large radius of curvature in combination with a smaller impeller exit width improves the flow along the shroud. As a result, flow separation is reduced, the flow leaving the impeller is more uniform and less turbulent, and the low-frequency noise is reduced. The flow in the fan casing also contributes to the low-frequency noise: here the flow along those parts of the volute that are close to the impeller periphery, i.e., the region close to the cutoff, is important.

Nomenclature

A	= cross-sectional area, $A_0 = 1$ m^2
a_0	= speed of sound
b_2	= impeller exit width
c	= absolute flow velocity
D	= impeller diameter
d	= duct or pipe diameter
d_{jet}	= jet diameter
f	= frequency
L_p	= pressure level relative to 20 μPa
L_W	= sound power level relative to 1 pW
Ma_0	= jet exit flow Mach number, u_0/a_0
n	= impeller speed
n_q	= specific fan speed, $157.8\,\varphi^{0.5}/\psi^{0.75}$
P	= sound power
P_{el}	= electric power of drive motor
p	= static flow pressure
Q	= volume flow, $Q_0 = 1$ m^3/s
Sr	= Strouhal number based on pipe diameter, fd/U
U	= impeller tip speed
u	= flow velocity
u_0	= jet exit flow velocity
Z	= number of impeller blades
z	= axial distance from impeller backplate
γ^2	= coherence function
Δp_{stat}	= static fan pressure
Δp_t	= total fan pressure, $\Delta p_{t0} = 1$ Pa
Δr	= radial distance from impeller periphery
δ	= cutoff clearance
η_t	= approximate total fan efficiency, $\Delta p_t Q_0/P_{\text{el}}$
θ	= circumferential angle
ρ_0	= air density
φ	= flow coefficient, $4Q/\pi D^2 U$
ψ	= pressure coefficient, $2\Delta p_t/\rho_0 U^2$

I. Introduction

AN experimental study is described to investigate the generation mechanisms of low-frequency centrifugal fan noise. More detailed descriptions of the research work, which was supported by the German Bundesminister für Wirtschaft (AIF 8396/9351) and the Forschungsvereinigung für Luft- und Trocknungstechnik, are given by Fehse[1] and Neise and Fehse.[2] Low-frequency noise in the region 20–200 Hz is relevant to air-conditioned rooms, clean rooms in particular, because it affects the well-being and the productivity of people working there. The generation mechanisms of these low-frequency room vibrations are not known yet; however, the assumption is made that they are produced by the fan interacting with the acoustic characteristics of the room. Centrifugal fans are known to be more problematic in this respect than axial-flow fans because their sound spectrum exhibits maximum levels in the low-frequency end.

II. Experimental Approach

The working hypothesis of the present study is that the low-frequency noise of centrifugal fans is generated by flow separations in the impeller and/or the casing, at least in the case when the noise is not dominated by inlet flow distortions or inlet turbulence. This hypothesis is based on the results of a paper by Stahl and Argüello,[3] who investigated the sound field in a circular pipe generated by a concentric jet flow entering the pipe through a convergent nozzle. The pipe diameter was $d = 100$ mm; different nozzle diameters were used in the study, but only the case $d_{\text{jet}} = 30$ mm is considered here. In Fig. 1 wall-pressure spectra, which were measured at an axial location 11 pipe diameters downstream of the exit plane of the nozzle ($x/d = 11$), are shown. Three cases are compared: in the first the air flow enters the pipe through the convergent nozzle only; in the second a short diffuser of length $L = d$ and wall angle $\varepsilon = 3$ deg is attached to the nozzle; and in the third the diffuser half angle is $\varepsilon = 7$ deg. In all three cases the mass flow entering the pipe is kept constant; the flow Mach number in the nozzle constriction is $Ma_0 = u_0/a_0 = 0.3$.

Addition of a diffuser lowers the velocity of the jet flow entering the pipe, and as a result the sound pressure level in the duct is reduced. In the case of the shallow diffuser angle $\varepsilon = 3$ deg, this is true for the entire frequency range measured, whereas for the diffuser angle $\varepsilon = 7$ deg an increase in sound pressure level of as much as 15 dB compared to the nozzle-only spectrum is observed at frequencies below 300 Hz. According to the results of many experimental studies, which were summarized by Klein,[4] flow separation occurs in the 7-deg diffuser but not in the 3-deg diffuser. This is a clear hint that the low-frequency-level increases are caused by the separated flow regimes in the 7-deg diffuser. It is emphasized at this point that the sound levels produced by the separated shear layer along the diffuser wall are higher than the ones generated by the free shear layer of the jet flow emanating from the convergent nozzle.

Presented as Paper 98-2370 at the AIAA/CEAS 4th Aeroacoustics Conference, Toulouse, France, 2–4 June 1998; received 10 June 1998; revision received 12 February 1999; accepted for publication 19 February 1999.

*Scientist, Institut für Antriebstechnik Abteilung Turbulenzforschung; currently Acoustic Engineer, TRW Fahrwerksysteme GmbH & Co. KG, Hansaallee 190, 40547 Düsseldorf, Germany.

†Head of Division, Institut für Antriebstechnik, Abteilung Turbulenzforschung, Müller-Breslau-Straße 8.

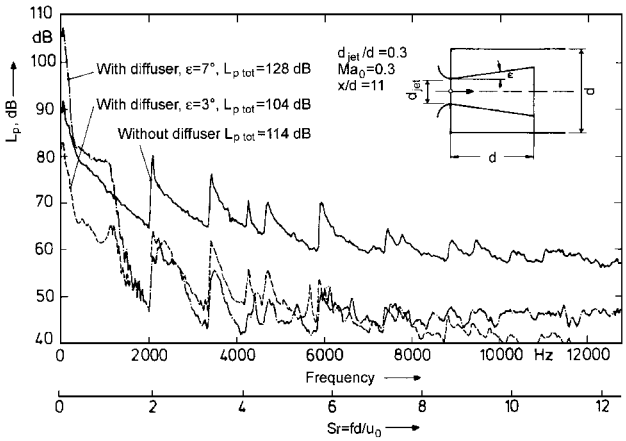

Fig. 1 Wall-pressure spectra in a circular pipe generated by a concentric jet flow (after Stahl and Argüello[3]).

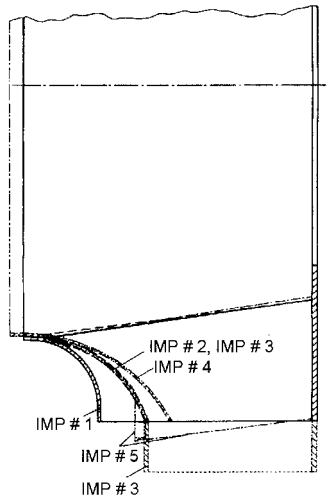

Fig. 2 Schematic presentation of the test impellers.

III. Description of Experimental Facilities

Centrifugal fans with backward curved blades were used for the experiments because the low-frequency noise problem occurs more often and more severely when this fan type is used. The aerodynamic performance of the test fans is characterized by specific speed values in the range $n_q = 80$–100. This fan type is commonly used for room ventilation and air-conditioning systems, and in the recent past problems with low-frequency noise have frequently been reported. Figure 2 shows schematically the five test impellers that are operated in the same fan casing. Impellers 1 and 2 of outer diameter $D = 406$ mm differ in their axial widths and in their shrouds' radius of curvature. The blades of impeller 1 are parallel to the axis of rotation throughout their radial extent, whereas the blade trailing edges of impeller 2 are sloped circumferentially, which involves a weakly three-dimensional blade curvature. Impeller 3 is constructed from impeller 2 by the addition of a rotating diffuser with constant axial width and 30-mm radial length to the outer circumference. The design of impeller 4 is characterized by the largest radius of curvature of the shroud and the smallest axial width at the outer periphery. Impellers 1–4 have airfoil-shaped backward curved blades and the same overall axial width; the same intake nozzle is used for these four impellers. A different nozzle has to be used for impeller 5, which has a slightly larger overall width. Also, the blades are made from flat sheet metal. The outer diameter of the shroud is larger than that of the backplate, and thus the blade trailing edges are inclined in the radial direction, as is shown in Fig. 2.

A schematic of the experimental setup is depicted in Fig. 3. The test fans are operated in a ducted-inlet/free-outlet installation. An anechoically terminated test duct is connected to the fan inlet for both the case impeller alone and the case impeller running in a casing. The casing has a conventional logarithmic spiral contour and parallel side walls; the cutoff clearance is $\delta = 50$ mm $= 0.25\,D/2$.

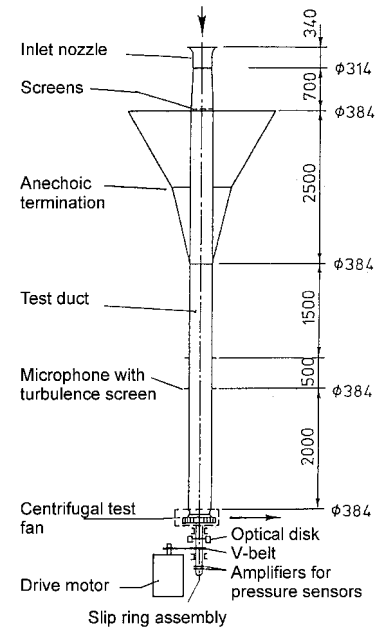

Fig. 3 Experimental facility (dimensions in millimeters).

The volume flow is determined via the static pressure in the inlet nozzle and the fan pressure rise via the static pressure in the test duct relative to the ambient pressure. Screens mounted just upstream of the anechoic duct termination are employed to control the fan operating condition. Steady flow pressures were acquired using electronic pressure transducers with a measurement uncertainty of $\pm 1\%$.

Sound measurements in the fan inlet duct are made in accordance with ISO 5136 (Ref. 5); however, in deviation from the standardized measurement procedure, only a single measurement position at the specified radial distance from the axis is used because only the low-frequency sound pressures, which propagate as plane waves, are of interest here. Furthermore, application of the various frequency corrections prescribed in the standard is omitted here because absolute sound power levels are not of interest but only level differences between different test configurations. The day-to-day and run-to-run repeatability of all pressure level measurements was observed to be within ± 1 dB.

For determination of the sound power radiated from the fan outlet side, the free-field method ISO 3744 (Ref. 6) is employed; the environmental correction and the background noise correction are not accounted for, for reasons similar to those of the in-duct measurements.

Unsteady wall-pressure measurements are made at various locations within impellers 1 and 2. Miniature pressure sensors (Kulite Semi-Conductor Type LQ47-5SG) are attached to the surfaces of the blades, the impeller shroud, and the backplate; the measurement positions are depicted in Fig. 4. The transducer leads are fed through the hollow fan shaft to two electronic circuit boards mounted on the shaft where the transducer signals are amplified before transmission into the fixed laboratory frame of reference via slip rings.

The pressure fluctuations on the casing wall are measured by using conventional static-pressure taps, which are connected to $\frac{1}{4}$-in. (6.35-mm) condenser microphones by means of specially made coupling devices.

Hot-wire measurements were made at the exit of impellers 1 and 2 using constant-temperature anemometry. Individual hot-wire probes were calibrated against a pitot tube in a free jet flow environment with a measurement uncertainty within $\pm 3\%$.

IV. Results

A. Comparison of Total Sound Power with and Without Fan Casing

Comparative measurements of the total sound power emitted with and without casing are made to assess the relative importance of the flowfields in the impeller and the casing for the low-frequency noise components. However, this comparison is meaningful only if the flow processes in the test impeller are essentially unaffected by the presence of the casing. Note that the stationary inlet nozzle that reaches into the impeller shroud is connected to the inlet duct

and remains in place when the fan casing is removed. In this way the leakage flow through the radial gap between inlet nozzle and shroud, which is driven by the pressure difference between the fan casing or, respectively, the impeller outlet, is retained. This gap flow is crucial for the aerodynamic performance of the impeller in that it supplies kinetic energy to the curved boundary-layer flow along the impeller shroud.

In Fig. 5 the aerodynamic performance curves of test impeller 2 are shown for the cases with and without spiral casing. For the latter case two curves are shown. When the dynamic pressure at the impeller outlet is based on the volumetric flow velocity $\bar{c} = Q/A$, i.e., $p_{dyn} = \rho_0 \bar{c}^2/2$, a much smaller total fan pressure is obtained without casing than with casing. When the dynamic pressure is determined by averaging the kinetic energy of the flow over the impeller exit area, i.e., $p_{dyn} = \rho_0 \overline{c^2}/2$, the total fan pressure for the casingless impeller is higher than with casing. The remaining differences between the two cases can be explained by the flow losses in the fan casing and by the fact that the dynamic pressure at the casing exit is still underestimated by considering only the volumetric velocity. Also, the leakage flow just mentioned may be somewhat different in the cases with and without casing because the driving pressure difference between inside and outside the inlet nozzle may be slightly different. In summary, we concluded that for this particular fan type the flow in the impeller is not much affected by the presence of the casing, and, therefore, comparing the noise production of these two configurations is meaningful.

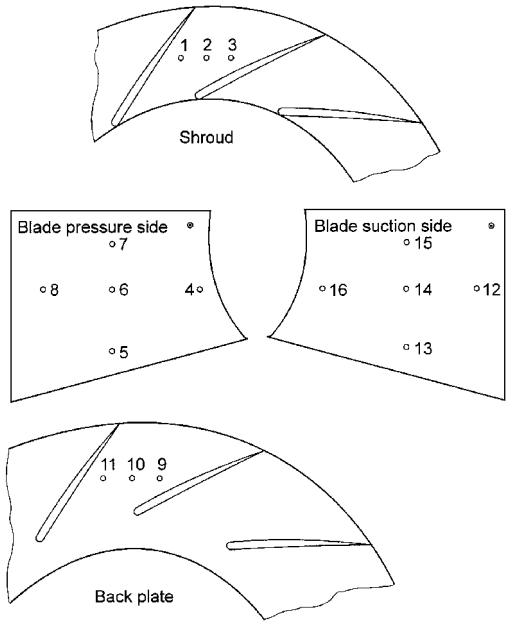

Fig. 4 Locations of pressure transducers in test impeller 1.

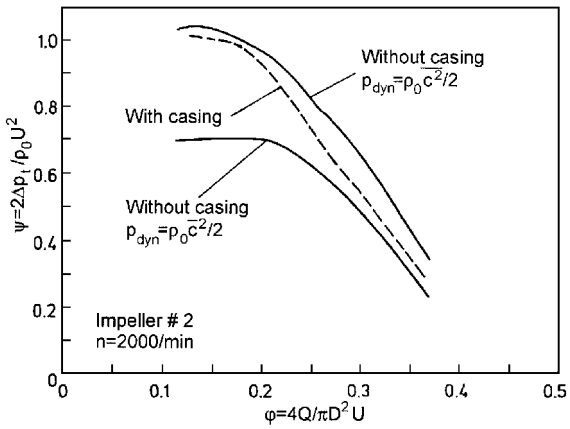

Fig. 5 Comparison of the aerodynamic fan performance curves of impeller 2 with and without casing; n = 2000/min.

Comparative sound measurements with and without casing are made for test impellers 1 and 2 for three operating conditions each: the flow rate of maximum efficiency φ_{opt}, $\varphi \approx 0.7\,\varphi_{opt}$, and $\varphi \approx 1.3\,\varphi_{opt}$. Some general observations from the experimental results are as follows. Addition of the casing naturally increases the blade tone levels because these components are mainly generated by the interaction of the flow leaving the impeller with the cutoff. However, it is the low-frequency random noise components that are of interest here, not the tonal components. For the random components the presence of the casing results in a redistribution of sound power from the outlet side to the inlet side of the fan. As a result, the sound power on the outlet side generated by the impeller with casing is lower than that of the impeller alone. This statement applies for all operating conditions measured and for both test impellers.

In the low-frequency range (20–200 Hz) the total sound power, i.e., the sum of inlet and outlet sound power, is increased by the presence of the fan casing. (See the spectra measured for impeller 2 at optimum fan operation, which are shown on the right-hand side of Fig. 6.) The same trend is observed for the other two operation conditions $\varphi \approx 0.7$ and $1.3\,\varphi_{opt}$ of both impellers 1 and 2, the only exception being impeller 1 at optimum operation. (See the diagram on the left-hand side of Fig. 6.) The conclusion to be drawn from the comparative sound power measurements is that the flow processes in the casing do contribute to the noise production of centrifugal fans; however, the level differences with and without casing do not indicate a dominating influence of either the impeller or the casing, and hence both the flow in the impeller and the casing have to be considered when searching for source areas of low-frequency fan noise.

B. Aerodynamic Fan Performance Curves

Figure 7 shows the aerodynamic fan performance curves of the five test impellers. The fan efficiency η is determined only approximately by measuring the electric power P_{el} of the drive motor; the electric motor efficiency was not accounted for. The highest total pressure is produced by impeller 3, which is equipped with the rotating diffuser at the outer periphery, and the best efficiency data are obtained with impellers 2–4.

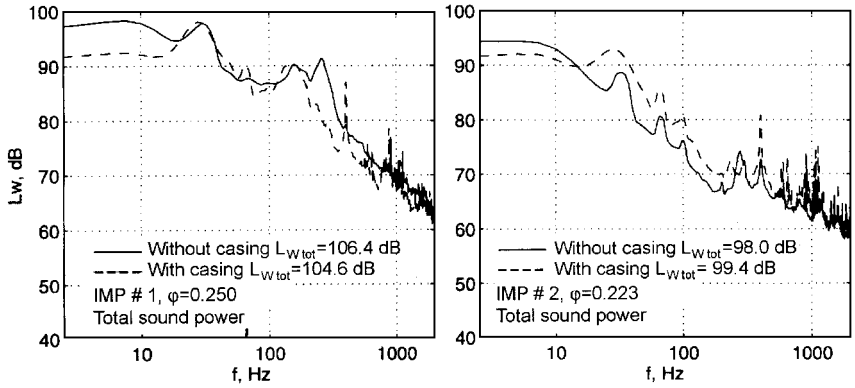

Fig. 6 Total sound power spectra of test impellers 1 and 2 with and without casing; φ_{opt}; n = 2000/min.

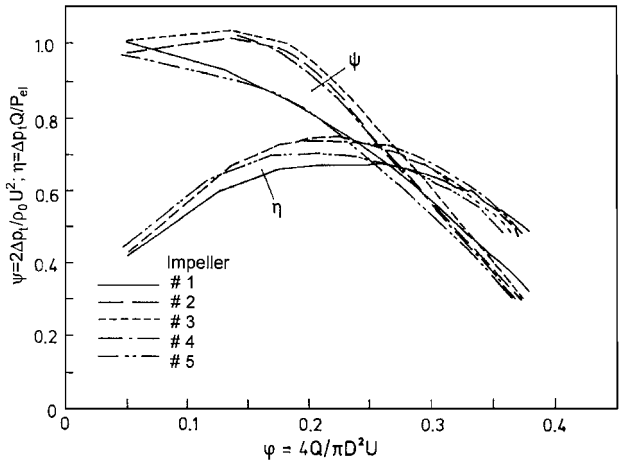

Fig. 7 Aerodynamic fan performance curves of five impellers operated in the same casing; $n = 2000$/min.

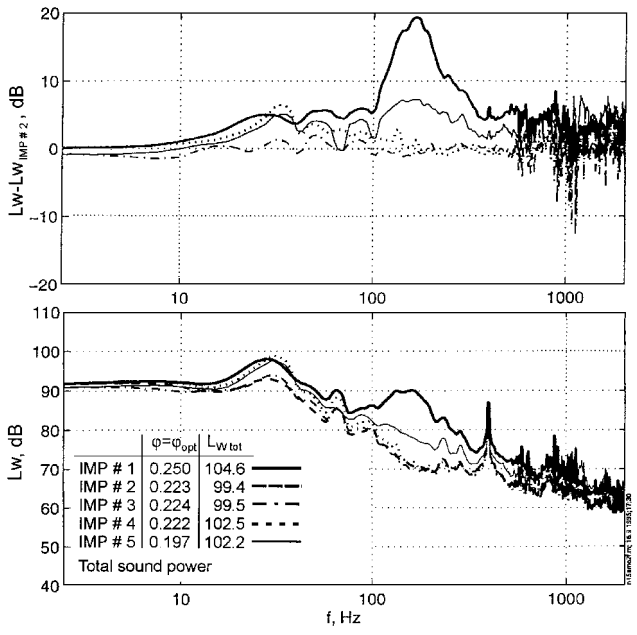

Fig. 8 Comparison of the total sound power spectra of test impellers 1–5; φ_{opt}; $n = 2000$/min.

C. Sound Power Spectra Measured in the Acoustic Far Field

Spectra of the total sound power (sum of inlet and outlet power) are shown in the bottom diagram of Fig. 8 for the five test impellers depicted in Fig. 2. To enhance the level differences between the various impeller designs, the sound power spectra relative to that of impeller 2 are plotted in the upper diagram of Fig. 8 in an expanded scale. The largest level reductions in the frequency range 20–400 Hz are observed when changing the geometry from impeller 1 to 2. Addition of the rotating diffuser (impeller 3) does not further reduce the low-frequency noise components. Making the impeller even smaller axially than impeller 2, combined with a further enlarged radius of curvature of the shroud, has no beneficial effect on the noise, which indicates that there is an optimum axial width in combination with a suitable shroud design.

At this point reporting an experimental finding by Gottschalk[7] is worthwhile: the smaller the axial width of the impeller, the higher the percentage of the flow going through the radial gap between the stationary inlet nozzle of the fan and the rotating impeller shroud. This gap flow provides energy to the boundary-layer flow along the shroud and, thereby, helps prevent or delay flow separation in this region. On the other hand, the smaller the axial width, the larger the relative displacement effect of the boundary layers along the shroud and backplate and, as a result, the smaller the region of sound core flow in the blade passage. The preceding two effects are the reason that reducing the axial width of the impeller improves the aerodynamic performance only up to a certain limit, and a similar reasoning obviously applies to the low-frequency noise generation. Finally, the low-frequency noise level of impeller 5 lies between those of impellers 1 and 2.

In conclusion, we note that impeller designs 1 and 2 showed the most significant differences in the low-frequency noise emission. Therefore, the decision was made to concentrate the investigation of the blade-pressure fluctuations on these two impeller designs. Moreover, to save testing time, casing wall pressures are measured only for the impeller with the highest low-frequency noise level, i.e., impeller 1.

D. Hot-Wire Measurements at the Impeller Exit

For the case with fan casing, spectra of the absolute flow velocity fluctuations measured at five axial locations across the impeller width at a radial distance of $\Delta r = 1\text{ mm} = 0.005\ D/2$ from the impeller periphery are plotted in Fig. 9. The spectra shown represent the average over four circumferential positions ($\theta = 0$, 90, 180, and 270 deg). Clearly, impeller 1 produces the highest turbulence levels and impeller 2 the lowest throughout the frequency range shown and at almost all measurement positions. Impeller 5 lies between the other two, similar to its noise characteristic; compare the sound spectra depicted in Fig. 8.

Circumferential profiles of the absolute flow velocity at the exit of impellers 1 and 2 are shown in Fig. 10. These profiles were obtained by phase averaging the signal of a stationary hot-wire probe over 100 revolutions. The range of the abscissa 0–0.03 s corresponds to one impeller revolution at $n = 2000$/min. Note that the peaks in the velocity profiles mark the wakes of the blades because in case of backward curved blades the absolute velocity vector becomes maximum when the relative velocity is minimum. The suction sides of the blades are located to the right of the peaks. Because of the phase averaging, the velocity profiles reveal characteristic differences between individual blade channels. For example, the blip in the second blade channel from the right of impeller 1 (upper diagram) is caused by a balancing weight mounted on the impeller backplate.

Near the backplate ($z/b_2 = 0.03$), the absolute velocity downstream of impeller 1 is small, i.e., the relative velocity is high, which is an indication that the flow conditions in the impeller blade channel are sound. The opposite is true for the region near the shroud ($z/b_2 = 0.91$), i.e., there the flow is heavily separated, in particular on the blade suction sides.

Flow separation can also be observed in the velocity profiles of impeller 2; however, they are limited to the immediate neighborhood of the blade suction side. The peaks in the velocity profiles measured near the shroud and the backplate are slightly shifted horizontally because the blade trailing edges are inclined relative to the rotational axis. A dramatic difference in the velocity profiles of impellers 1 and 2 is observed on the shroud side. Obviously, the lower curvature of the shroud of impeller 2 provides a better guidance of the flow turning from the axial into the radial direction and, hence, has a positive effect on the flow conditions in the blade channels. As a result, the flow leaving the impeller is more uniform and less turbulent, and the noise generation is diminished.

E. Pressure Fluctuations on the Impeller Walls

Examples of the spectra of the wall-pressure fluctuations on the shroud of impeller 1 are depicted in the upper diagram of Fig. 11; compare the measurement positions shown in Fig. 4. The diagram in the middle gives the coherence between the flow pressures measured on the shroud and the acoustic pressures in the fan inlet duct, and in the bottom diagram the coherent part of the shroud pressures is plotted. Determination of the coherent part of a signal is discussed in more detail in the book by Bendat and Piersol[8] and for the present application specifically in the papers by Fehse[1] and Neise and Fehse.[2] The spectral spikes at 33.3 Hz and harmonics are caused by the shaft rotation and are not of interest here, only the random components, which are caused by the turbulent flow in the impeller.

Because the spectral distribution of the coherent flow pressures varies with measurement position, it is difficult to rank the various impeller regimes with respect to their importance for low-frequency

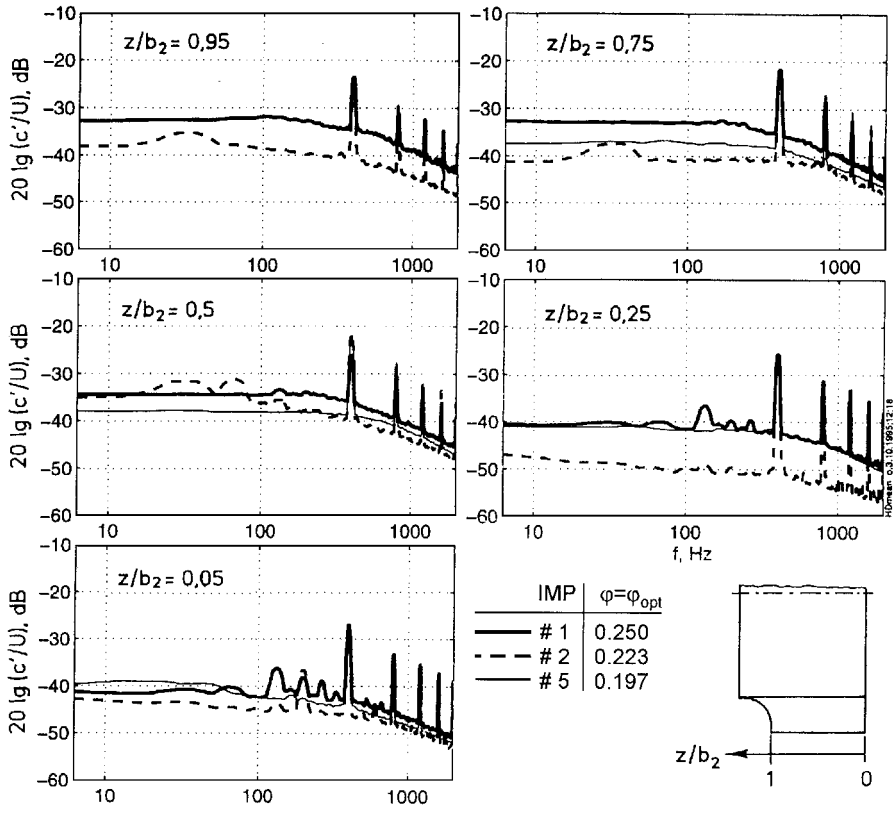

Fig. 9 Spectra of the absolute velocity fluctuations at the exit of impellers 1, 2, and 5 ($\Delta r = 1$ mm $= 0.005D/2$); spectra averaged over four circumferential positions ($\theta = 0$, 90, 180, and 270 deg); impellers with casing; $\varphi = \varphi_{opt}$; $n = 2000$/min.

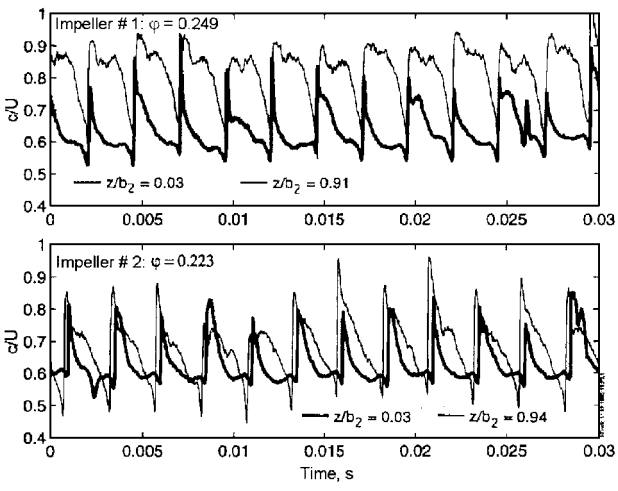

Fig. 10 Circumferential profiles of the absolute flow velocity at the exit of impellers 1 and 2; $\Delta r = 1$ mm $= 0.005D/2$; $\varphi = \varphi_{opt}$; $n = 2000$/min.

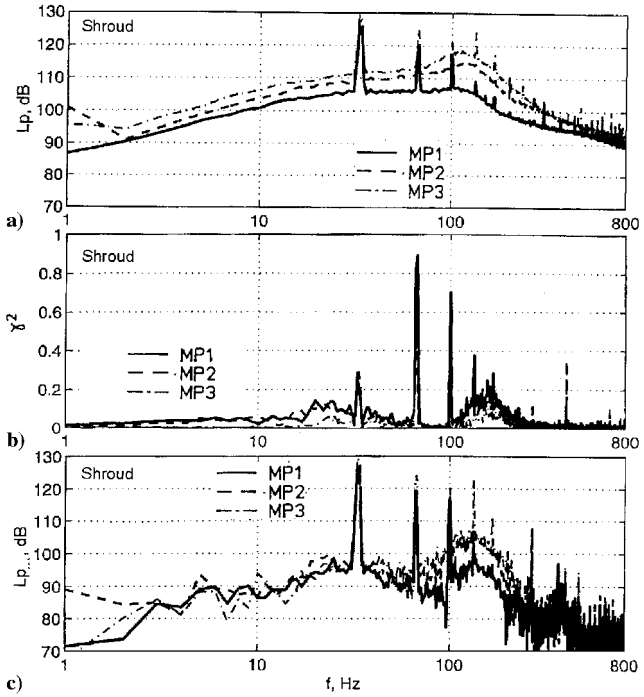

Fig. 11 Spectra of a) wall-pressure fluctuations in impeller 1, b) coherence between wall pressures and acoustic pressures in the inlet duct, and c) coherent part of wall pressures; $\varphi_{opt} = 0.250$; $n = 2000$/min.

noise generation. Therefore the shaft rotation spikes were eliminated from the spectra, and an integral value of the random components was computed for the frequency range 0–800 Hz. The result is shown in Fig. 12 for all measurement points of impellers 1 and 2. There is a striking difference between the coherent levels of the two impeller designs at all three flow rates tested. The largest differences occur on the shroud, on the portion of the blade pressure side that is close to the shroud (MP 4; compare Fig. 4), and on the blade suction sides. This observation is a clear indication for the importance of these areas within impeller 1 for the generation of low-frequency noise.

Similar coherence analyses were carried out involving the wall pressures in the impeller and the acoustic far-field pressures on the outlet side. The outcome is as just described; i.e., the ranking of the various source areas is the same as when the acoustic pressures in the inlet duct are used as a reference.

A general experimental observation from the study of wall pressures in the two fan impellers is that high random levels go together with low coherence with the far-field acoustic pressures and vice versa.

The conclusion to be drawn from the just-described experiments is that a substantial portion of the low-frequency noise of centrifugal fans is caused by classical flow separation areas within the impeller, i.e., the blade suction sides, the shroud, and the adjacent portions of the blades. This statement is strictly true only for the inlet flow conditions in the present experiments, which are governed by a

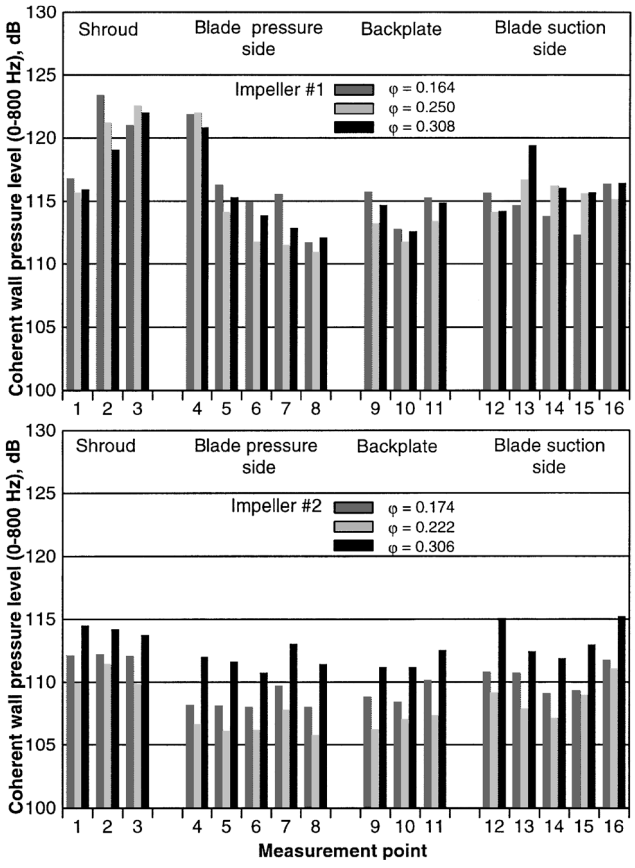

Fig. 12 Level $\langle L_{p\ coh}\rangle_{0-800\ Hz}$ of impeller wall pressures coherent with the acoustic far-field pressures in the inlet duct in the frequency range 0–800 Hz without periodic components; n = 2000/min.

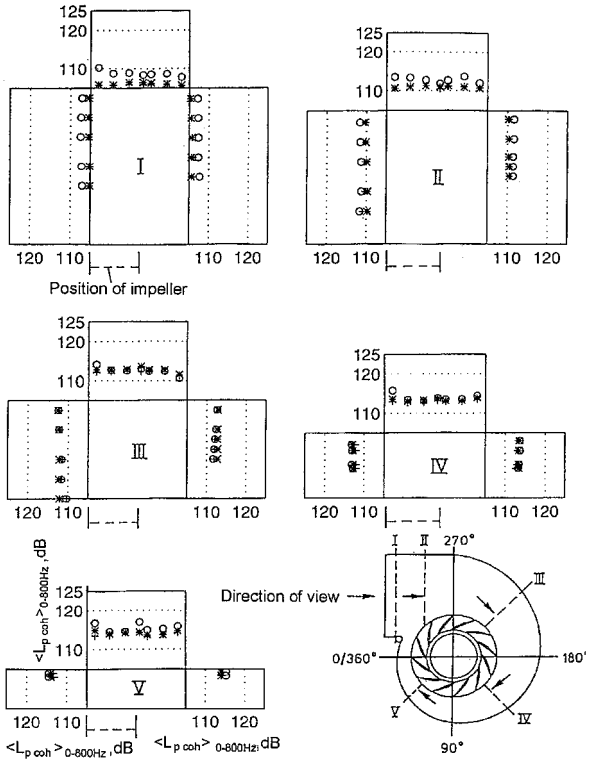

Fig. 13 Level $\langle L_{p\ coh}\rangle_{0-800\ Hz}$ of the casing wall pressures coherent with the acoustic far-field pressures on the outlet side in the range 0–800 Hz without periodic components: impeller 1, n = 2000/min; **, $\varphi = 0.164$; ++++, $\varphi_{opt} = 0.250$; and ∘∘∘∘, $\varphi = 0.308$.**

6500-mm (17 duct diameters)-long straight circular inlet duct. The mean flow profile can be assumed to be nearly fully developed with turbulence intensities of about 3% on the axis and close to 10% near the duct wall (compare Ref. 9). It has been shown experimentally[10] that centrifugal fans are fairly insensitive to inlet flow disturbance and turbulence in their noise generation characteristics, so that one can conclude that the preceding statement on the importance of the flow separation regions for low-frequency centrifugal fan noise applies for most inlet flow conditions encountered in practice.

F. Wall Pressures in the Fan Casing

Unsteady pressures on the casing walls were measured only for impeller 1. The measurement points are distributed along the intersecting lines of the fan casing walls with the five planes I–V, which are indicated in the legend of Fig. 13, where the level of the coherent wall pressures in the frequency range 0–800 Hz with the harmonic components removed from the spectrum is plotted; the acoustic free-field pressure on the outlet side is used as a reference signal. The rectangles marked I to V indicate the free cross section between the casing side walls (vertical lines), the volute (upper horizontal line), and the impeller outlet (bottom horizontal line). The coherent pressure level on the casing wall is plotted vertical to the corresponding line of each rectangle. Results are given for three fan operating conditions.

The highest coherent wall-pressure levels are found in plane V from where they decrease toward the fan outlet. In this plane the direct wall pressure levels are also highest.

G. Interaction Between Impeller Flow and Casing Flow

In this section we attempted to illustrate the interaction between the flow leaving the impeller and the flow in the fan casing. On the left-hand side of Fig. 14 are plotted the levels of the random wall pressures on the spiral casing in the frequency bands 64–448 Hz and 448–704 Hz as functions of the azimuthal angle θ (compare

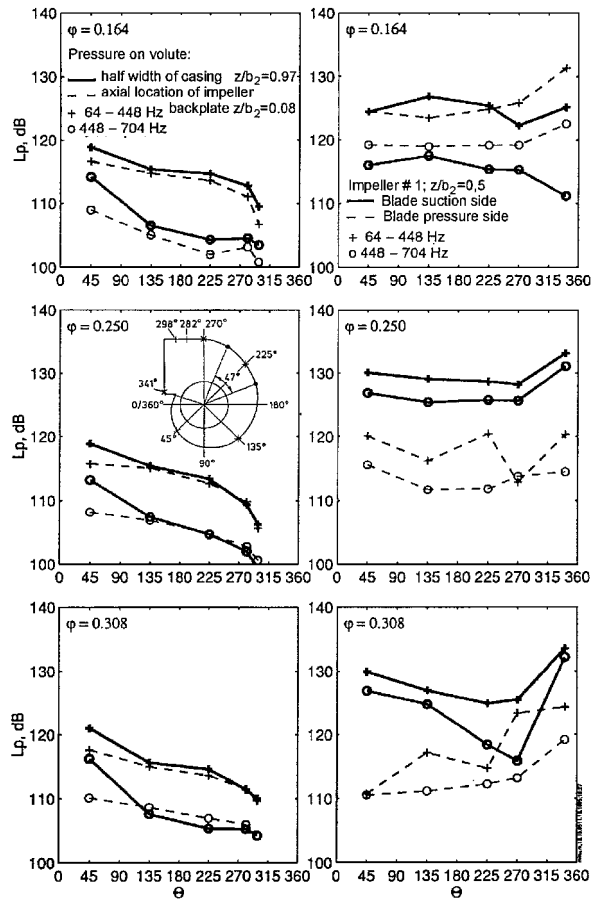

Fig. 14 Level of broadband wall-pressure components measured on the volute and the impeller blades: impeller 1, n = 2000/min.

the sketch of the fan in the legend). The two bands cover the frequency range, which is of interest here. The three stacked diagrams are for three fan operating conditions. For each angular location measurements were made at two axial positions, $z/b_2 = 0.08$ near the impeller backplate and $z/b_2 = 0.97$ about midway between the casing side walls. For all three fan operation conditions and for both axial measurement locations, the low-frequency wall-pressure level decreases with the azimuthal angle, i.e., with increasing distance of the spiral wall from the impeller.

On the right-hand side of Fig. 14 are shown the levels of the same two spectral components measured on the suction side and pressure side of the impeller blades at an axial position halfway between shroud and backplate. Again, the spectral components are shown as functions of the azimuthal angle, i.e., the angular position of the impeller blade. Each measurement point represents the average over an angular span of $\Delta\theta \approx 47$ deg, which is schematically shown in the legend of Fig. 14. The center of each angular span is marked with an asterisk, i.e., the azimuthal angles $\theta = 45, 135, 225, 270$, and 341 deg.

The spiral casing influences the flow pressures exerted on the impeller blades although the cutoff clearance of the test fan is relatively large, $\delta = 0.25\, D/2$: when approaching the cutoff regime, the blade pressure level rises sharply. The pressures on the impeller blades are always substantially higher than on the spiral wall. Except for $\varphi = 0.164$, the levels on the blade suction side are higher than on the pressure side, which once again emphasizes the importance of this source regime.

V. Conclusions

An experimental study is described to explore the generation mechanisms of the low-frequency random noise of centrifugal fans. Low-frequency noise in the range 20–200 Hz is a frequent practical problem in air-conditioned rooms, in particular clean rooms, because it affects the health and well-being of people in these rooms.

Experiments were made with five industrially manufactured test impellers having different geometries. The aerodynamic characteristics of the test fans are described by specific speed values in the range $n_q = 80$–100. All test impellers have backward curved blades and are run in one and the same casing. A 17-duct-diameter-long straight circular duct was mounted on the fan inlet side.

Comparison of the total sound power spectra emitted by the different impeller designs led to the conclusion that, up to a certain point, a smaller axial impeller width at the outer periphery in combination with a larger radius of curvature of the shroud has a positive effect on the generation of low-frequency sound. This statement holds for flow rates in the range of 70–130% of the optimum one. Particularly large level differences were observed between two designs (compare impellers 1 and 2 in Fig. 2), for which subsequently more detailed investigations were carried out. Lower sound levels were obtained with impeller 2, which is narrower axially at the outer circumference than impeller 1 and has a more gradually curved shroud.

Hot-wire measurements showed that the turbulence intensity of the flow at the exit of impeller 2 is in fact significantly lower than that of impeller 1. Spectra of the velocity fluctuations taken at a close distance from the impeller periphery exhibit much lower levels in the low-frequency regime for impeller 2; this is true for all axial measurement positions but particularly so near the impeller shroud. The circumferential velocity profiles across one impeller channel, i.e., across two blades, indicate that in the case of impeller 1 there are large regions of separated flow along the blade suction side, which in the case of impeller 2 are much less pronounced. This observation supports the preceding findings.

The larger radius of curvature of the shroud of impeller 2 is obviously beneficial for the mean flow turning from the axial into the radial direction and as a result for better flow conditions in the blade channels.

Cross-correlation experiments involving the unsteady wall pressures in the test impellers and the sound pressure in the acoustic far field led to the following ranking of the various source regions: 1, impeller shroud; 2, blade suction sides; 3, backplate; and 4, blade-pressure sides. When impellers 1 and 2 are compared, the largest differences in the coherent levels are found on the shroud, on the portion of the blade-pressure side, which is close to the shroud, and on the blade suction sides. Thus, the cross-correlation analysis has revealed that the low-frequency noise of centrifugal fans is produced by classical flow separation areas on the impeller shroud and blade suction sides. This statement is believed to be true for most inlet flow conditions encountered in practice, i.e., when inlet flow distortion noise or inlet turbulence noise is not dominating.

Cross-correlation analyses were also made to investigate the importance of the casing wall pressures for the low-frequency noise components. The cutoff area and adjacent parts of the volute ($\theta \approx -19$–180 deg) are relevant for the generation of low-frequency noise for two reasons: first, the coherent wall-pressure levels are highest in this area, and second, the presence of the spiral wall influences the upstream flow in the impeller channels and increases the fluctuating wall pressures there.

In conclusion, we note that the design of the impeller is most important for reducing the low-frequency noise of centrifugal fans. The shroud geometry plays a particularly important role. A small radius of curvature gives rise to flow separations, which result in nonuniform flow conditions and high turbulence intensities within the impeller as well as in the casing. With a lower shroud curvature, a better guidance of the flow turning from the axial into the radial direction is achieved, which improves the flow conditions in general, and as a result noise generation is diminished. The blade design should try to avoid flow separation, which is most likely to occur on the suction side, to minimize low-frequency noise.

Acknowledgments

The authors would like to thank the companies Gebhardt Ventilatoren, Waldenburg; Ziehl Abegg, Künzelsau; and Siemens A. G., Bremen for supplying the test fans and drive.

References

[1] Fehse, K.-R., "Experimentelle Untersuchungen zur Entstehung tieffrequenter Druckschwankungen bei Radialventilatoren," Ph.D. Dissertation, Fachbereich 6 (Verfahrenstechnik, Umwelttechnik, Werkstoffwissenschaften; Chemical Engineering, Environmental Sciences, Material Sciences), Technische Univ., Berlin, June 1997.

[2] Neise, W., and Fehse, K.-R., "Entstehungsursachen tieffrequenter Druckschwankungen bei Radialventilatoren II (Abschlußbericht zum AIF/FLT-Vorhaben Nr. 9351)," Forschungsvereinigung für Luft- und Trocknungstechnik e.V., FLT 3/1/78/95, Frankfurt/Main, Germany, Nov. 1995.

[3] Stahl, B., and Argüello, G., "Schallerzeugung und Schalldämpfung in einer Rohrströmung stromab einer unstetigen Querschnittserweiterung," *Acustica*, Vol. 65, No. 2, 1988, pp. 75–84.

[4] Klein, A., "Review: Effects of Inlet Conditions on Conical-Diffuser Performance," *Journal of Fluids Engineering*, Vol. 103, No. 2, 1981, pp. 250–257.

[5] "Determination of Sound Power Radiated Into a Duct by Fans—In-Duct Method," International Standard, International Organization for Standardization, ISO 5136, Geneva, Dec. 1990.

[6] "Acoustics—Determination of Sound Power Levels of Noise Sources Using Sound Pressure—Engineering Method in an Essentially Free-Field over a Reflecting Plane," International Standard, International Organization for Standardization, ISO 3744, Geneva, May 1994.

[7] Gottschalk, M., "Untersuchung der Kennlinienstetigkeit von Radialventilatoren," *Strömungsmechanik und Strömungsmaschinen*, Heft 17, Mitteilungen des Inst. für Strömungslehre und Strömungsmaschinen der Univ. Karlsruhe, Karlsruhe, Germany, 1974, pp. 1–40.

[8] Bendat, J. S., and Piersol, G., *Engineering Applications of Correlation and Spectral Analysis*, Wiley, New York, 1980, Chaps. 4 and 9.

[9] Laufer, J., "The Structure of Turbulence in Fully Developed Pipe Flow," NACA TR-1174, 1954.

[10] Neise, W., "Installation Effects on Fan Noise," *Proceedings of the European Conference on Installation Effects in Fan Systems*, Inst. of Mechanical Engineers, London, 1990, pp. 83–91.

A. Plotkin
Associate Editor